**Signal Localization of Variable Intensity, Thin, Curved Lines in Noisy Images.** N. T. Dutton[1], M. A. Mendlovitz[1], F. S. Turner[1], G. W. Patterson[1], [1]The Johns Hopkins University Applied Physics Laboratory; Laurel, MD (nicholas.dutton@jhuapl.edu).

**Introduction:** Many problems in digital signal processing, specifically image processing and computer vision, require object identification of curved lines. Examples include medical imaging applications such as x-ray angiograms, Intelligence Surveillance and Reconnaissance applications for finding roads and rivers, and – in the particular case of this work – finding the direct-path signal in bistatic Synthetic Aperture Radar (SAR) pulse-compressed data (i.e., waterfall plots).

Signal localization of lines in noisy imagery is a broad topic. Edge detection techniques such as the Sobel or Canny operators [1], and feature extraction techniques such as the Hough transform [2] exist and are well represented in literature, however with large datasets they can often be computationally expensive and also require customization for the specific application. This fine tuning can become cumbersome and time consuming especially when the imagery content significantly varies between datasets.

To mitigate some of these issues, a general purpose solution to isolating thin, curved lines of variable shape and intensity in imagery that includes complexly structured noise is presented, followed by an example application using bistatic SAR data in which the approach was used with good results.

**Problem Statement:** The problem presented is to create an algorithm that will automate finding and fitting of a vertical, thin, curved line of varying intensity and shape in the presence of structured noise. For this application, the vertical, thin, curved line represents the direct-path signal from a ground station transmitting through the back of the Mini-RF antenna. The following is a list of constraints on the waterfall plots:

1) The structured noise in the imagery may cross the direct-path throughout the image. When this occurs the direct-path intensity may be less than, equal to, or greater than the crossing noise source at different pixels within the crossing region. 2) A minimum of two structured noise sources are present in the imagery, but there may be others. 3) The direct-path may not be visible in portions of the image. 4) The imagery may have horizontal strips where no data exists. 5) The structured noise may also be similar in shape and intensity of the direct-path.

**Solution Approach:** The direct-path is usually distinguishable from the structured noise sources to the trained eye. One is inclined to recreate a similar process by which a human locates this thin line in the imagery.

First, we seek an algorithm to find the "sharpest" vertical spike in a subset of the imagery. The magnitudes of the columns of the imagery data are summed to get an intensity count across the horizontal axis, $I(x)$. An average intensity count is then computed in a buffer window, $I_{avg}(x \pm \Delta x_{buffer})$, on each side of every element in $I(x)$. The index, $x$, with the highest ratio of the peak intensity value to the average buffer intensity, $I(x)/I_{avg}(x \pm \Delta x_{buffer})$, is the sharpest spike. This is the direct-path's estimated location in the horizontal axis. Using this buffered average approach reduces the likelihood that a signal will be selected purely because it is bright and selects thin vertical lines in the image over thicker ones.

Second, a maximum horizontal boundary should be established over all datasets which represents the maximum deviation of the direct-path in the horizontal direction. This maximum horizontal span, $\Delta x_{max}$, limits the total amount of data in the imagery that needs to be assessed and helps minimize the likelihood of selecting a false signal as the direct-path.

Third, a rectangular subsection of the image is taken, centered horizontally at the initial estimate of the direct path and spans $\pm\Delta x_{max}/2$ horizontally, and an amount $\Delta y$ in the vertical direction. $\Delta y$ should be chosen such that the direct-path can be assumed to have little to no curvature over that region. The direct path $x$-axis location is estimated within the rectangular subsection using the algorithm discussed in the first step. The estimated coordinates are then placed at the center of the $y$-dimension of the subsection.

Fourth, the rectangular subsection is slid down the image and the direct-path $x$-axis location is recomputed within the window as described in the first step. The coordinates are stored and this process is repeated until the full y-axis span of the image is covered. To ensure the vertical linearity assumption and to sample the pixels towards the end of the image, $\Delta y$ is allowed to shrink.

Finally, once the estimated $x$-$y$ coordinates of the direct-path are stored for the full vertical image strip, outliers must be checked to ensure the estimates do not drift radically. These outliers can occur if one of the structured noise sources in the image crosses the direct-path. The outliers are removed by checking that the angle between the neighboring direct-path pixel $x$ and $y$ coordinate estimates is approximately 90 degrees – i.e. a locally vertical direct-path. The direct-path estimated

locations can then be fit to an $n^{th}$ order polynomial and reapplied to the image as necessary.

**Application:** The Miniature Radio Frequency (Mini-RF) dual-polarized synthetic aperture radar (SAR) instrument aboard NASA's Lunar Reconnaissance Orbiter (LRO) is operated in concert with the Arecibo and DSS-13 observatories to collect bistatic radar data on the nearside of the lunar surface [3]. When processing the bistatic radar data, the direct-path signal is the signal received by Mini-RF directly from the observatory and is used to improve timing and phase reconstruction of the chirped signal.

Several factors make automating the isolation of the direct-path in pulse-compressed difficult. The Arecibo and DSS-13 observatories operate at different transmit powers and frequencies; 200kW in the S-band and 80kW in the X-band respectively. This leads to different signal strengths received by the radar and in general the direct-path may not be the strongest signal in the radar waterfall plot. The geometry and signal characteristics of the bistatic collect also influence the specular forward scatter and diffuse backscatter signal returns. Situations can arise where the direct-path signal overlaps the forward and/or backscatter (See Figure 1).

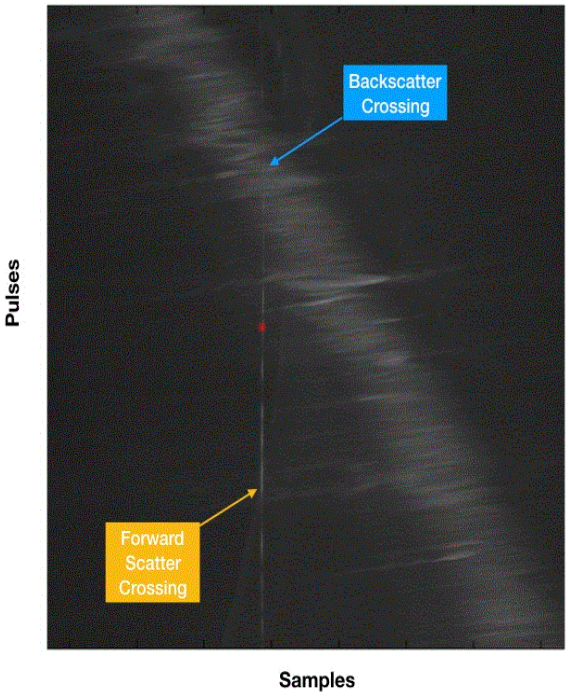


Figure 1. X-band Waterfall Plot

The algorithm described above is applied to the Mini-RF waterfall plots in order to locate the direct-path. The algorithm works well even for situations in which the forward scatter and backscatter cross the direct-path and mitigate, in most cases, the issues described in the problem statement. Figure 2 shows the algorithm's estimate of the direct path. The imagery is zoomed and centered on the direct-path to show its curvature. The 'x' marks are the direct-path estimate at the corresponding sample-pulse pair and the line connecting the 'x' marks is a $5^{th}$ order polynomial fit. Regions where the x's are sparse along the direct-path imply outliers were removed from the data. The overall fit still works well even if a large number of outliers are removed.

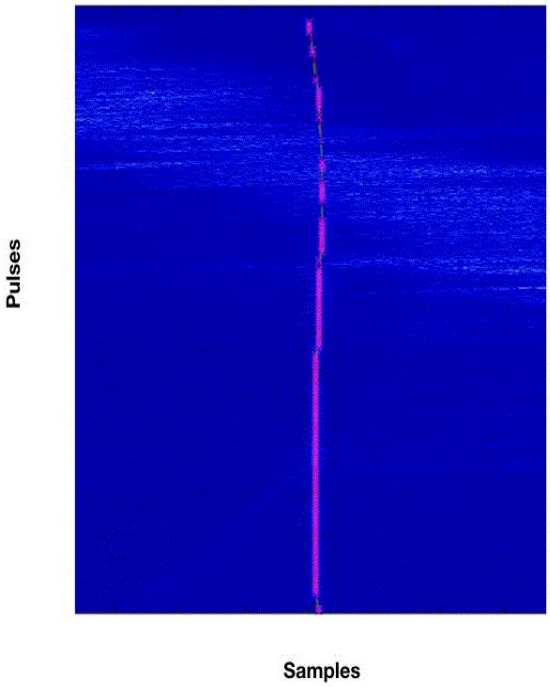


Figure 2. Direct-path Estimate and Fit

**Conclusions:** Previous image processing approaches were used to determine the location of the direct-path in the pulse-compressed data, but these approaches often required time-consuming techniques and manual intervention to locate the samples for each pulse corresponding to the direct path. The general approach discussed above presents a new automated approach in which approximately 95% of the Mini-RF collects do not require manual intervention - a significant improvement over previously used methods. Future work will attempt to isolate and resolve the issues associated with the remaining 5% of the Mini-RF collects which do require human intervention to find the direct-path.

**References:**

[1] Canny, J. (1986) IEEE. Vol. PAMI-8, *6*, 679-698;
[2] Duda, R. O. et al. (1972) Comm. ACM, *15*, 11-15
[3] Patterson G. W. et al. (2017) Icarus, *283*, 2–19.